

# Analysis of the Influence of Asymmetric Grid on Synchronous Hydro Generator

Hongbo Qiu, Xiaobin Fan\*, Jianqin Feng, and Cunxiang Yang

**Abstract**—In order to analyze the influence of three-phase asymmetrical operation of a generator on its stable operation, firstly, taking a 24-MW bulb turbine generator as an example, the 2-D transient electromagnetic field model is established. Through the comparison analysis of the experimental results and simulation data, the correctness of the model is verified. Secondly, the values of air gap flux density, torque and loss in different conditions are obtained by using the finite element method. The effects of asymmetric three-phase current on air gap flux density, torque and loss are determined. Thirdly, the corresponding relationships between the three-phase current unbalance degree and torque ripple, eddy current loss are established, and the variations of torque ripple and eddy current loss are given when the three-phase current unbalance degree is changed. The result shows that the asymmetry three-phase current makes the torque ripple and eddy current loss increase dramatically, which seriously threaten the safe and stable operation of the generator. Finally, the further study on the torque ripple and eddy current loss of the generator under different current distributions and the same three-phase unbalance degree identifies that the content of negative sequence current is a key factor to affect the torque ripple and eddy current loss.

## 1. INTRODUCTION

The asymmetrical operation of the synchronous hydro generator is inevitable in the process of operation. The generator structure is three-phase symmetrical, and its three-phase electromotive force is also symmetrical. So, the main factor that leads to the asymmetrical operation of the synchronous hydro generator is the asymmetry of three-phase current [1]. In real life, the existence of asymmetrical load, such as the electric locomotive in transportation, the electric furnace in metallurgical factory and the asymmetrical impedance of three-phase lines, leads to the generation of asymmetrical current in power grid [2–7]. Since the synchronous hydro generator is directly connected to the grid through the transformer, the influence of asymmetrical three-phase current on the generator is inevitable. The negative sequence current is existent in the armature windings when the generator is running at asymmetric condition, and it will affect the air-gap flux density, torques and eddy current loss of the generator. In recent years, the vibration of bulb turbine generator of the Chai J. X. hydropower station is serious [8, 9]. Fig. 1 shows the faults of the rotor that caused by vibration. Torque ripple is a main factor to cause generator vibration. Therefore, analyzing the torque ripple of the generator has a practical significance.

Some experts and scholars have carried out relevant researches on the asymmetrical operation of generator. In [10], a stand-alone wind-based dual-stator-winding induction generator is presented when the external load is asymmetrical. In [11], a new control system for unbalanced operation of induction generator is proposed. The experimental results show that the proposed control system has excellent

---

*Received 16 August 2017, Accepted 11 October 2017, Scheduled 6 November 2017*

\* Corresponding author: Xiaobin Fan (fanxiaobin66@163.com).

The authors are with the College of Electric and Information Engineering, Zhengzhou University of Light Industry, Zhengzhou, Henan, China.

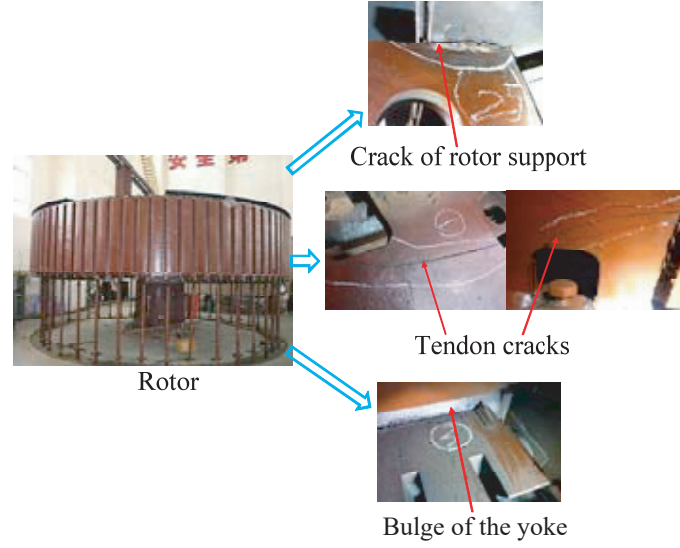


**Figure 1.** Faults caused by vibration.

performance. However, the study about the air gap magnetic field, torque and the change mechanism of the loss in damper bars when the generator is running at asymmetrical state is less. The energy conversion between stator and rotor is realized by the air gap magnetic field. The torque ripple and average torque of generator are respectively related to the stable operation and load capacity. The eddy current loss of the damper bars is the main loss of the generator, which directly determines the efficiency of the generator. Therefore, the study about the air gap flux density, torque and eddy current loss is extremely essential.

In this paper, a bulb turbine generator is taken as an example. According to the generator size, the transient electromagnetic field model of the generator was established by using finite element software. The various parameters were calculated based on finite element method. The variations of torque ripple and eddy current loss of the generator were studied when the generator was running at different conditions. At the same time, the electric current density distribution of the damping bars was also analyzed.

## 2. TWO-DIMENSIONAL MODEL OF THE GENERATOR

The research object of this paper is a 24-MW bulb turbine generator, and its model type is SFWG24-88/7820. For SFWG24-88/7820, the stator connection type is YY. An insulation class of the generator is F. The pole core is assembled by magnetic steel WDEL235. Some main parameters of the generator are shown in Table 1.

Considering the symmetry properties of generator, the generator can be divided into 22 units.

**Table 1.** Parameter values of the generator.

| Parameters                | value  | Parameters                | value |
|---------------------------|--------|---------------------------|-------|
| Rated power /MW           | 24     | Stator inner diameter /mm | 7370  |
| Rated voltage /kV         | 10.5   | Length of stator core /mm | 1350  |
| Rated current /A          | 1388.9 | Number of stator slots    | 462   |
| Rated speed (r/min)       | 68.18  | Conductors per slot       | 2     |
| Stator outer diameter /mm | 7820   | Number of poles           | 88    |

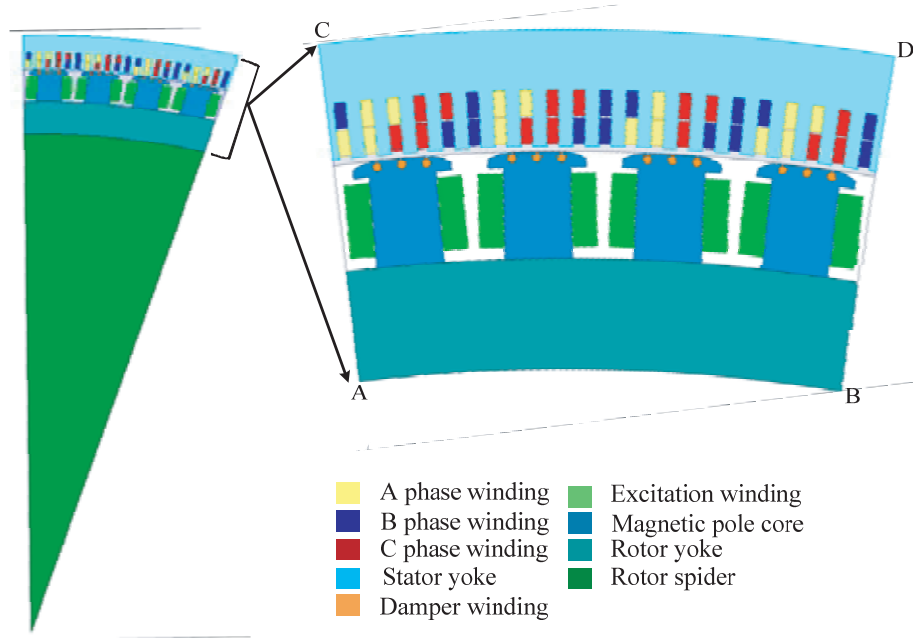


**Figure 2.** 2-D electromagnetic analysis model of the generator.

Therefore, according to the generator data of size, materials, rated parameters, etc., a unit generator model is established by using finite element software. The 2-D electromagnetic model of a unit generator is shown in Fig. 2. The triangulation algorithm was adopted to analyze the generator model. The number of mesh elements is 39003.

For analyzing the mathematic model of electromagnetic field of the generator, the boundary conditions of the model are given [17]:

$$\begin{cases} \frac{\partial}{\partial x} \left( \nu \frac{\partial A_z}{\partial x} \right) + \frac{\partial}{\partial y} \left( \nu \frac{\partial A_z}{\partial y} \right) = -J_z + \sigma \frac{dA_z}{dt} \\ A|_{AB} = A|_{CD} = 0 \\ A|_{AC} = A|_{BD} \end{cases} \quad (1)$$

where  $\mu$  is the material permeability;  $A_z$  is the  $Z$  axis component of magnetic vector potential  $A$ ;  $J_z$  is the  $Z$  axis component of current density;  $\sigma(dA_z/dt)$  is the eddy current density.

In order to verify the correctness of the model, the electromagnetic field distribution and operational characteristics of the generator were analyzed. When the generator was running at rated state, the distribution of the magnetic flux density was provided, as shown in Fig. 3.

When the generator is running at various conditions, the operation characteristic parameters can be obtained through calculations. When the generator project was completed through assembly, a series tests had been made to evaluate the quality of the engineering, such as short-circuit test, test without load, test with load, DC voltage endurance test, and AC voltage endurance test.

The operating characteristic curves of the generator were drawn according to the simulation results and experimental data, as shown in Fig. 4. In the figure, the horizontal coordinate is the value of the excitation current; the longitudinal coordinate on the left side is the induced phase voltage in the armature winding; the longitudinal coordinate on the right side is the armature current.

Figure 3 shows that the magnetic field distribution of the generator is in agreement with the theory. Through analysis of the data in Fig. 4, it can be known that the error between the simulation and experiment is within 7%, which meets the requirements of engineering research. Through the above analysis, the correctness of the model is verified.

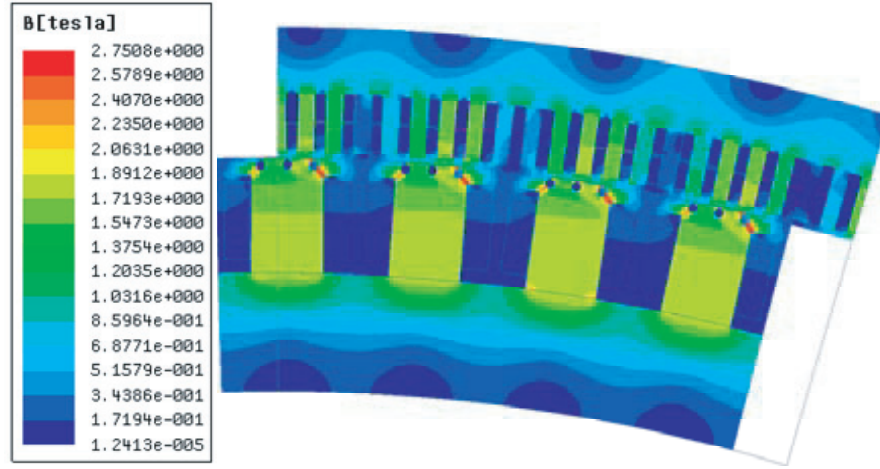


**Figure 3.** Magnetic flux density distribution.

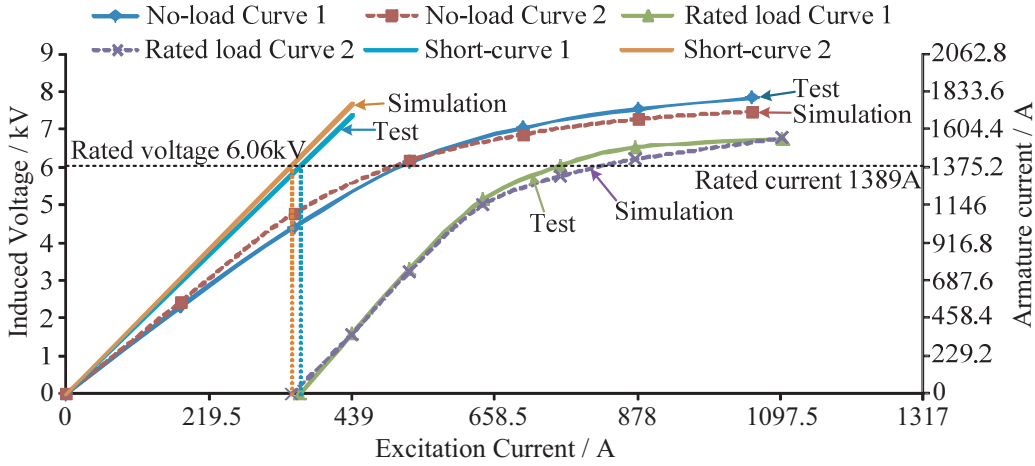


**Figure 4.** Operation characteristic curves.

### 3. ANALYSIS ON THE STATE OF ASYMMETRIC OPERATION OF GENERATOR

Affected by external factors, it is inevitable that the generator was operated at asymmetrical state. The asymmetrical operation of the generator will result in the increase of torque ripple and decrease of power generation efficiency. The electromagnetic field of the generator under an asymmetrical condition is analyzed in Fig. 5.

In the figure,  $\dot{I}_A$ ,  $\dot{I}_B$ ,  $\dot{I}_C$  are the phasors of three-phase current in the armature winding;  $\dot{I}_{A0}$ ,  $\dot{I}_{A+}$ ,  $\dot{I}_{A-}$  are the components of zero, positive and negative sequence current phasors;  $\alpha$  is the vector operator.

Three-phase asymmetrical operation of the generator includes long term three-phase asymmetric operation state and short term three-phase asymmetrical operation state. Long term three-phase asymmetrical operation is caused by unbalanced three-phase load and impedance of transmission lines. Short term three-phase asymmetrical operation is mainly caused by the non-full phase operation of power grid or generator.

Three-phase asymmetric operation is caused by the asymmetrical three-phase current. And the three-phase current unbalance degree is a characteristic parameter to measure the degree of asymmetrical

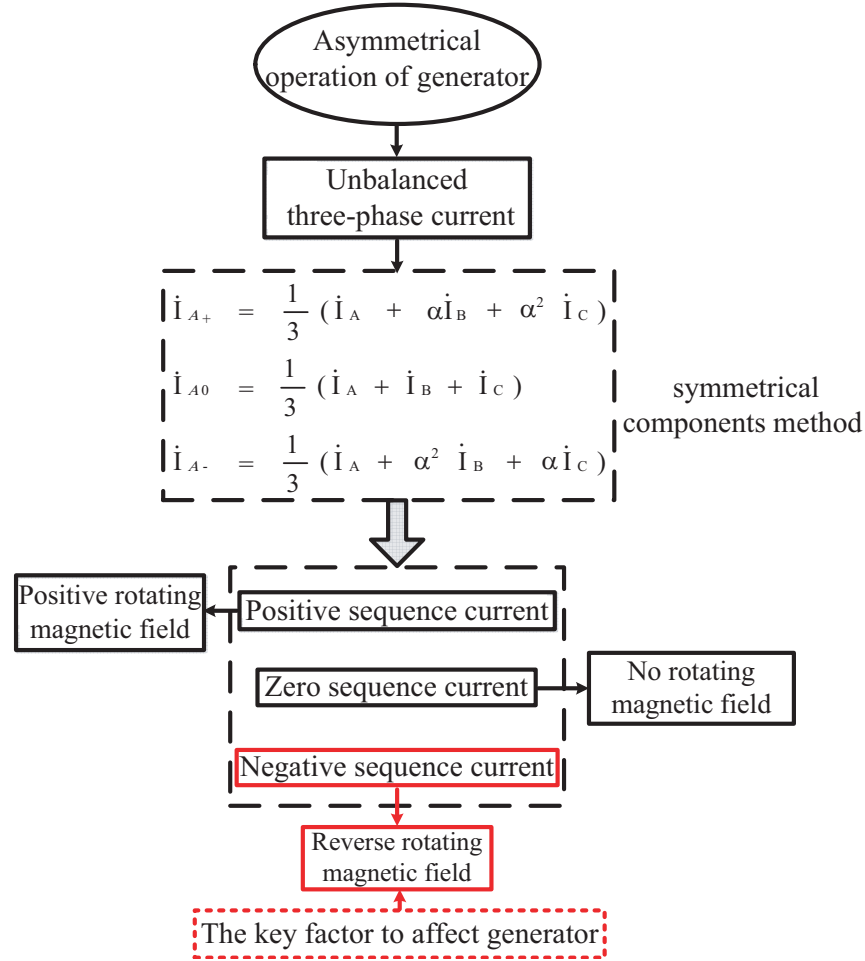


**Figure 5.** Electromagnetic field analysis.

three-phase current. The calculation method used in this paper is shown in Formula (2) [12].

$$\text{LUCR}\% = (\max(\text{abs}(I_i - I_{\text{avg}})/I_{\text{avg}})) * 100\% \quad (2)$$

where, LUCR% is the three-phase current unbalance degree;  $I_{\text{avg}}$  is the average value of three-phase current;  $I_i$  corresponds to the valid values of  $I_A$ ,  $I_B$  and  $I_C$ , and  $I_A$ ,  $I_B$  and  $I_C$  denote the RMS values of the phase A, B and C currents.

In this paper, keep the average current of three-phase current as a constant, that is, under the condition of the output power basically unchanged. The characteristics of the generator were studied in the following three kinds of asymmetrical conditions. In order to facilitate the analysis, the operation states of the generator were assumed as follows:

The first state: Three phase currents are equal ( $I_A = I_B = I_C$ );

The second state: Two phase currents are equal and less than the third phase current ( $I_A > I_B = I_C$ );

The third state: Two phase currents are equal and more than the third phase current ( $I_A < I_B = I_C$ );

The fourth state: Keep one phase current as a constant, changing the currents of the other two phase currents ( $I_A > I_C > I_B$ ).

When the short circuit faulted, non-full phase operation state or any other abnormal conditions occurred in the power system, which would cause the asymmetrical operation of the generator. Once the generator is running at asymmetrical state, there will be negative sequence current in the armature winding. The magnetic field generated by the negative sequence current will cut the damping bars at

two times of the synchronous speed, and then generate double frequency eddy current in the damping bars. Although the generator could withstand a certain negative sequence current, its existence could cause a series of problems, such as loss increase, rotor temperature rise and torque ripple increase.

#### 4. ANALYSIS OF THE EFFECTS OF ASYMMETRIC OPERATION ON THE GENERATOR

##### 4.1. The Influence of the Asymmetrical Operation of the Generator on the Air Gap Magnetic Field

Air-gap flux density is an important parameter of synchronous generator [13, 14]. The air gap magnetic field of the generator is composed of main pole magnetic field and armature magnetic field. For a star-winding generator, when the generator is running at asymmetrical condition, the armature magnetic field is formed by positive sequence magnetic field and negative sequence magnetic field.

Fig. 6 shows the magnetic flux density distributions of the generator when the generator is running at asymmetrical condition, and the current unbalance degree are 6% and 12%, respectively. .

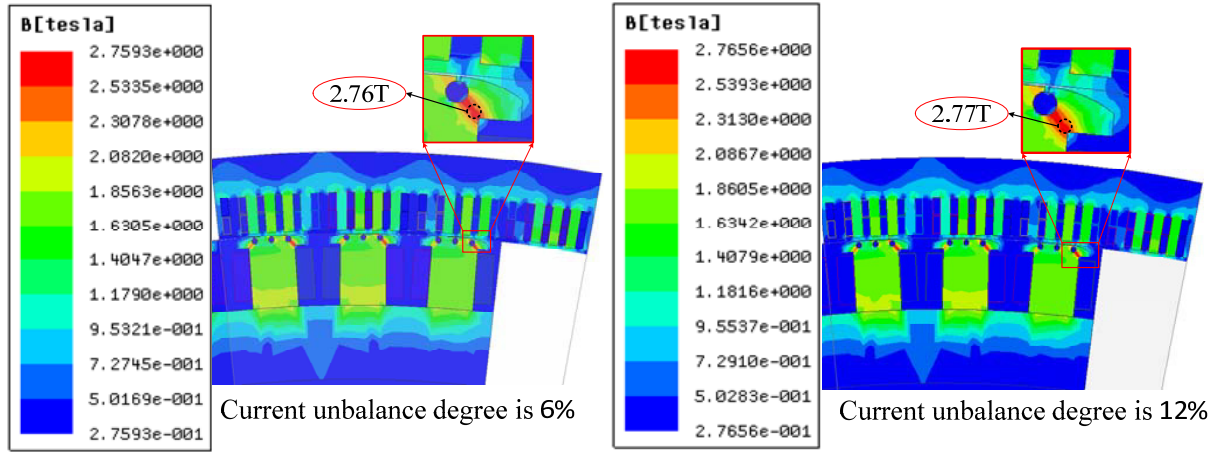


**Figure 6.** Magnetic flux density distribution of the generator.

From Fig. 6, it can be seen that the difference of the magnetic flux density distribution of the generator between these two situations is not obvious. When the current unbalance degree increases from 6% to 12%, the change value of the maximum magnetic flux density is 0.01 T.

Due to the influence of main pole magnetic field and armature magnetic field, the effect of negative sequence current is not obvious. Therefore, the negative sequence component is individually analyzed in the following part. It means that the influences of magnetic field and armature magnetic field on the generator are neglected. Taking the generator operating at the fourth state ( $I_A > I_C > I_B$ ) as an example, the air gap flux density distributions of the generator are analyzed when the current unbalance degree are 6% and 12% respectively. The air gap flux density distributions of the generator at different conditions are shown in Fig. 7.

Figure 7 shows that the magnetic flux density generated by the negative sequence current increases obviously when the generator is running at unbalanced state, and the current unbalanced degree is increased from 6% to 12%. The difference of the magnetic flux density of the generator under these two conditions is about two times larger. The magnetic field in the generator is unsaturated when the impacts of the main pole magnetic field and armature magnetic field are neglected.

From the above analysis, it can be known that the intensity of the magnetic field generated by the negative sequence current increases linearly with the increase of the current unbalance degree when the magnetic saturation is not considered. However, the relationships between the magnetic field intensity



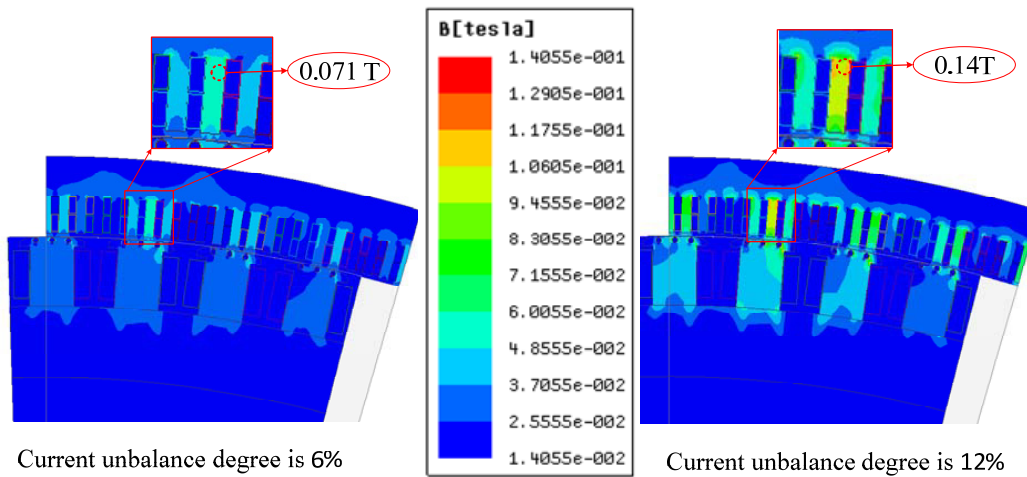


**Figure 7.** Magnetic flux density distribution of the generator only when the negative sequence current is considered.

and torque as well as the magnetic field intensity and eddy current loss are nonlinear. Therefore, the influences of the asymmetrical operation of generator on the torque and eddy current loss are more complicated, which are studied in detail in the following part.

#### 4.2. The Influence of the Asymmetrical Operation of the Generator on the Torque

A circular rotating magnetic potential can be generated in the air gap when the symmetrical three-phase current exists in the symmetrical three-phase windings. However, when the three-phase current is asymmetrical, the synthesized magnetic potential in the generator is composed by positive rotation magnetic potential and reverse rotation magnetic potential.

The size of the synthesized magnetic potential is periodic, and the frequency is two times of the rated frequency. The torque produced by the synthetic magnetic potential is also periodic, and the frequency of the alternating torque is 100 Hz. From above analysis, it can be known that the existence of negative sequence magnetic field will increase the generator vibration and even cause metal fatigue and mechanical damage. The torque waveforms of the generator at rated operation and asymmetrical operation ( $I_A > I_C > I_B$ ) are analyzed, as shown in Fig. 8.

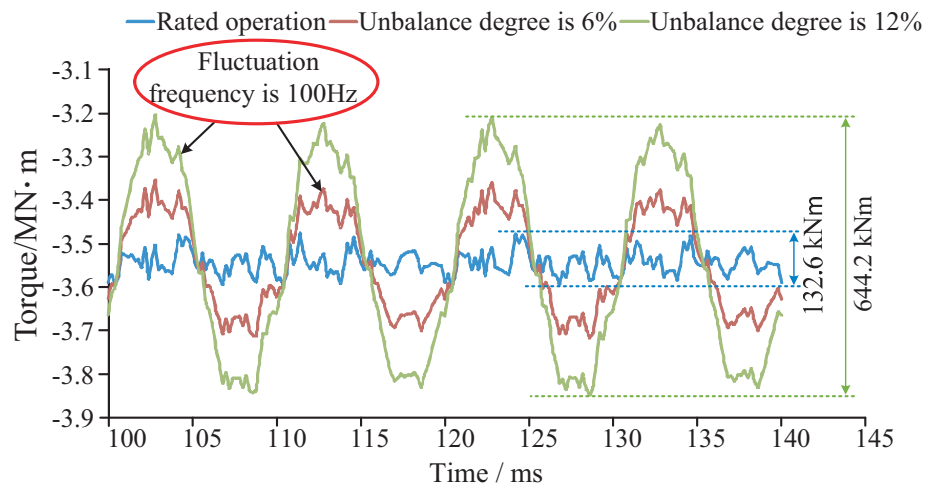


**Figure 8.** Torque waveforms of the generator.

Figure 8 shows that the torque ripple is small, and the variation is not obvious when the generator is running at rated condition. However, when the generator is running at asymmetrical condition, the generator torque is markedly increased. The torque ripple is periodic, and the fluctuation frequency is 100 Hz. When the three-phase current unbalance degree is 12%, the torque ripple is increased by 3.8 times compared with the rated condition. Through the above analysis, it can be known that the asymmetrical operation has a great impact on the generator torque.

The variations of the torque with three-phase current unbalance degree were analyzed when the generator was running at asymmetric conditions. Since the step selection of the finite element method will have a certain effect on the results of the torque, the sampling method was used to calculate the maximum, minimum and average values of the torque. The specific solutions are as follows:

- 1) When the generator was in stable operation, two periods torque waveform was selected for data acquisition.
- 2) Sort the collected data by size. Select five maximum and five minimum values, respectively, and their average values that were the maximum and minimum values of the torque.
- 3) The average torque of the generator can be gained by the mean value of all the values calculated by the software.

The data of the generator torque are obtained through the simulation, sampling and calculation, as shown in Table 2.

**Table 2.** Torque data of the generator.

| Unbalance degree | Torque (kNm)      |             |                   |             |                   |             |
|------------------|-------------------|-------------|-------------------|-------------|-------------------|-------------|
|                  | $I_A > I_B = I_C$ |             | $I_A < I_B = I_C$ |             | $I_A > I_C > I_B$ |             |
|                  | Torque ripple     | Avg. torque | Torque ripple     | Avg. torque | Torque ripple     | Avg. torque |
| 3%               | 213.9             | 3546.8      | 182.0             | 3546.9      | 216.5             | 3546.6      |
| 6%               | 334.1             | 3546.6      | 305.1             | 3546.9      | 339.4             | 3546.4      |
| 9%               | 454.1             | 3546.3      | 429.0             | 3546.8      | 476.5             | 3546.0      |
| 12%              | 575.9             | 3546.0      | 553.8             | 3546.6      | 616.4             | 3545.5      |

Notes: The torque ripple and average torque are 109.8 kNm and 3546.8 kNm, respectively, when the generator is running at rated condition.

From Table 2, it can be seen that the torque ripple of the generator is increased significantly when the current in the armature winding is asymmetrical. When the three-phase current degree is 3%, and the generator is running at these three kinds of asymmetrical states, respectively ( $I_A > I_B = I_C$ ,  $I_A < I_B = I_C$  and  $I_A > I_C > I_B$ ), the torque ripple is increased by 94.8%, 65.8% and 97.2%, respectively. The variation curves of the generation torque ripple with the three-phase current unbalance degree are given, as shown in Fig. 9.

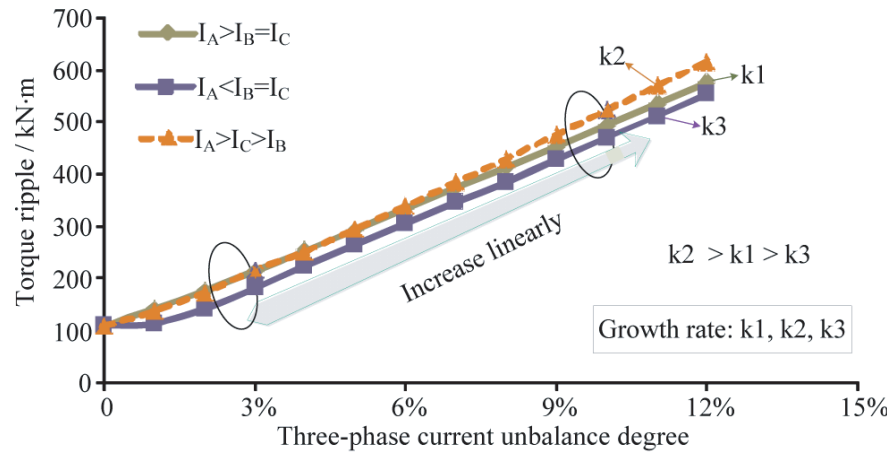
The average torque of the generator has a tendency to decrease with the increase of the negative sequence current. However, when the unbalance degree reaches 12%, a decrease in average torque is still less than 1‰. It shows that there is little influence on the average torque when the unbalance degree is within 12%.

Figure 9 shows that the torque ripple increases slowly when the unbalance degree is within 3%, but when the unbalance degree is more than 3%, the torque ripple increases linearly with the increase of three-phase current unbalance degree. The increase of the torque ripple is most obvious when the generator is running at the fourth state ( $I_A > I_C > I_B$ ).

For further analyze the changing mechanism of the torque ripple when the generator is running at asymmetrical states, the contents of negative sequence current in the armature winding under different conditions are calculated, as shown in Table 3.

Comparing Table 2 with Table 3, it can be known that the larger the negative sequence current is in the three-phase current, the greater the torque ripple is. When the unbalance degree is 12%, the





**Figure 9.** The curve of the torque ripple.

**Table 3.** The analysis of negative sequence current.

| Unbalance degree | Amplitude of negative sequence current (A) |                   |                   |
|------------------|--|-------------------|-------------------|
|                  | $I_A > I_B = I_C$                          | $I_A < I_B = I_C$ | $I_A > I_C > I_B$ |
| 3%               | 30.65                                      | 28.24             | 35.06             |
| 6%               | 60.09                                      | 57.68             | 69.06             |
| 9%               | 89.53                                      | 87.12             | 103.07            |
| 12%              | 118.98                                     | 116.57            | 137.08            |

content of the negative sequence current in these three kinds of asymmetrical states ( $I_A > I_B = I_C$ ,  $I_A < I_B = I_C$  and  $I_A > I_C > I_B$ ) are 6.06%, 5.94% and 6.98%, respectively. The change of negative sequence current content is corresponding to the change of the torque ripple. The above analysis shows that the negative sequence current is a key factor to affect the generator torque ripple.

### 4.3. The Influence of the Asymmetrical Operation of the Generator on the Eddy Current Loss

#### 4.3.1. Electric Current Density Distribution of the Damper Winding

The excitation regulator and the governor out of control or a fault occurring during the operation of the generator will cause the vibration of the generator. For reducing the occurrence of the above situations, damping bars were arranged on the rotor poles, which could restrain the vibration of the generator [15, 16]. However, when the negative sequence current exists in the armature winding, the eddy current loss will be affected.

The eddy current losses of the damper bars can be obtained by the following formula.

$$P_{\text{loss}} = \frac{1}{\sigma} \int_{\text{vol}} J^2 dV \quad (3)$$

where  $J$  is the current density;  $\sigma$  is the conductivity of the material;  $V$  is the volume of damper bars.

The distribution of the eddy current density is given in the following equation.

$$\vec{j} = \frac{\partial H}{\partial x} = -H_0 \frac{1+j}{\Delta} e^{-(1+j)\frac{x}{\Delta}} = -J_0 e^{-\frac{x}{\Delta}} e^{-(\frac{x}{\Delta} - 45^\circ)} \quad (4)$$

where  $J_0$  is the current density;  $H_0$  is the magnetic intensity;  $\Delta$  is the skin depth of the magnetic field;  $x$  is the skin depth of the current density.

When the generator is running at rated state, taking its electric current density distribution and eddy current loss as a reference, the variation of electric current density distribution of damping bars was analyzed with the unbalance degree 12%. The electric current density distribution of two sets of damping bars at different conditions is analyzed, as shown in Fig. 10.

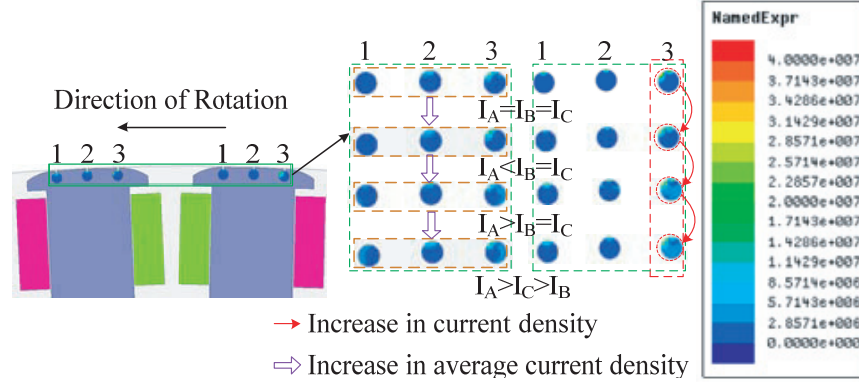


**Figure 10.** Electric current density distribution of damping bars.

From Fig. 10, it can be seen that the skin effect is obvious, and most of the eddy current is close to the damper slots. The electric current density of the damping bars is increased gradually when the generator is running at three kinds of asymmetric state respectively ( $I_A > I_B = I_C$ ,  $I_A < I_B = I_C$  and  $I_A > I_C > I_B$ ). When the generator is running at the fourth state ( $I_A > I_C > I_B$ ), the increase of the electric current density of the damping bars is the most obvious. In these three damping bars, damper bar 3 gathered most of the eddy current. This provides a new idea for the optimal design of the damping bars in generator.

#### 4.3.2. Analysis of the Eddy Current Loss

Eddy current density and eddy current loss are inseparable. Eddy current loss is the main loss of generator, which will affect the generator output power [17]. In order to further analyze the effect of the asymmetric operation of the generator on the eddy current loss, the detailed data about the eddy current loss of the generator under different operating conditions were obtained. The growth curves of eddy current loss with the unbalance degree are given in Fig. 11.

From Fig. 11, it can be known that with the increase of the unbalance degree, the increasing rate of eddy current loss is gradually increased. When the generator is running at these three kinds of

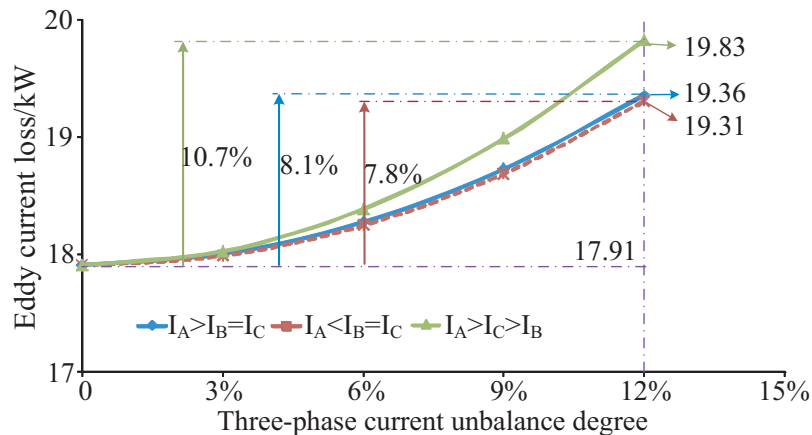


**Figure 11.** The curve of eddy current loss.

asymmetrical states respectively ( $I_A > I_B = I_C$ ,  $I_A < I_B = I_C$  and  $I_A > I_C > I_B$ ) and the unbalance degree is 12%, the eddy current loss of the damping bars are increased by 8.1%, 7.8% and 10.7%, respectively. Through the comparison of Table 3 and Fig. 10, it can be seen that the changes of the eddy current loss and negative sequence current content are consistent with each other. The above analysis further confirms that the negative sequence current is a substantive element to affect the eddy current loss.

## 5. CONCLUSION

In this paper, a 24-MW bulb turbine generator is taken as an example. The torque and eddy current loss of the generator under different conditions were analyzed by using finite element method. Through detailed analysis, the following conclusions are obtained.

- 1) When the generator is running at the rated state, the torque ripple is mainly affected by the slot harmonic magnetic field, and the variation is not obvious. When the generator is running at the asymmetric state, the magnetic field produced by the negative sequence current is the main factor to affect the torque ripple. The variation of the generator torque is periodic, and the frequency is 100 Hz.
- 2) The torque ripple increases nonlinearly with the increase of the three-phase current unbalance degree in general. The torque ripple increases slowly when the unbalance degree is less than 3%. However, when the unbalance degree is more than 3%, the torque ripple has a linear increasing trend. When the unbalance degree is 9% and the generator is running at these three kinds of asymmetric state respectively ( $I_A > I_B = I_C$ ,  $I_A < I_B = I_C$  and  $I_A > I_C > I_B$ ), the torque ripple is increased by 2.9 ~ 3.3 times compared to the rated operation.
- 3) Under the same unbalance degree, the torque ripples caused by these three kinds of asymmetrical operation are different. When the generator is running at the fourth state ( $I_A > I_C > I_B$ ), the torque ripple is 1 ~ 1.2 times of the other two states ( $I_A > I_B = I_C$  and  $I_A < I_B = I_C$ ).
- 4) The eddy current loss increases slowly when the unbalance degree is less than 6%. However, when the unbalance degree is more than 6%, the increasing rate of the eddy current loss is obviously increased. When the unbalance degree is 12% and the generator is running at these three kinds of asymmetrical state respectively ( $I_A > I_B = I_C$ ,  $I_A < I_B = I_C$  and  $I_A > I_C > I_B$ ), the eddy current losses of the generator are increased by 8.1%, 7.8% and 10.7%, respectively.

## ACKNOWLEDGMENT

This work was supported in part by the National Natural Science Foundation of China under Grant 51507156, in part by the University Key Scientific Research Programs of Henan province under Grant 17A470005, in part by the Doctoral Program of Zhengzhou University of Light Industry under Grant 2014BSJJ042, in part by the Major Science and Technology Special Projects of Henan Province under Grant 161100211600, in part by the Scientific and Technological Projects of Zhengzhou under Grant 20150442, in part by the Foundation for Key Teacher of Zhengzhou University of Light Industry, and in part by the Graduate Innovation Fund of Zhengzhou University of Light Industry under Grant 2016048.

## REFERENCES

1. Pei, X. J., W. Zhou, and Y. Kang, "Analysis and calculation of DC-link current and voltage ripples for three-phase inverter with unbalanced load," *IEEE Trans. Power Electron.*, Vol. 30, No. 10, 5401–5412, Oct. 2015.
2. Sezgin, E., M. Göl, and Ö. Salor, "State-estimation-based determination of harmonic current contributions of iron and steel plants supplied from PCC," *IEEE Trans. Ind. Appl.*, Vol. 52, No. 3, 2654–2663, Dec. 2016.
3. Vijayan, V. and S. Ashok, "High-performance bi-directional Z-source inverter for locomotive drive application," *IET Electr. Syst. Transp.*, Vol. 5, No. 4, 166–174, Dec. 2015.

4. Mwasilu, F., J. J. Justo, K. S. Ro, and J. W. Jung, "Improvement of dynamic performance of doubly fed induction generator-based wind turbine power system under an unbalanced grid voltage condition," *IET Renew Power Gener.*, Vol. 6, No. 6, 424–434, Nov. 2012.
5. Yan, R. and T. K. Saha, "Investigation of voltage imbalance due to distribution network unbalanced line configurations and load levels," *IEEE Trans. Power Del.*, Vol. 28, No. 2, 1829–1838, May 2013.
6. Woolley, N. C. and J. V. Milanovic, "Statistical estimation of the source and level of voltage unbalance in distribution networks," *IEEE Trans. Power Del.*, Vol. 27, No. 3, 1450–1460, Jul. 2012.
7. Esfahani, M. T. and B. Vahidi, "A new stochastic model of electric arc furnace based on hidden markov model: A study of its effects on the power system," *IEEE Trans. Power Del.*, Vol. 27, No. 4, 1893–1901, Oct. 2012.
8. Song, H. B. and Z. G. Li, "Alteration of cognate curve and its influences on bulb tubular turbines," *Journal of Gansu Sciences*, Vol. 22, No. 4, 145–149, Dec. 2010 (in Chinese).
9. Song, H. B., W. L. Li, and F. Y. Yang, "Placement angle effect of axial and radial stent on ventilation structure in bulb tubular turbine," *Journal of Jiangsu University (Natural Science Edition)*, Vol. 34, No. 3, 281–286, May 2013 (in Chinese).
10. Moradian, M. and J. Soltani, "An isolated three-phase induction generator system with dual stator winding sets under unbalanced load condition," *IEEE Trans. Energy Convers.*, Vol. 31, No. 2, 531–539, Jun. 2016.
11. Peña, R., R. Cárdenas, E. Escobar, J. Clare, and P. Wheeler, "Control system for unbalanced operation of stand-alone doubly fed induction generators," *IEEE Trans. Energy Convers.*, Vol. 22, No. 2, 544–545, Jun. 2007.
12. Singh, S. B., A. K. Singh, and P. Thakur, "Accurate performance assessment of IM with approximate current unbalance factor for NEMA definition," *Int. Conf. Harmonic and Quality of Power*, 674–678, 2014.
13. Yu, Q., X. S. Wang, and Y. H. Cheng, "Determination of air-gap flux density characteristics of switched reluctance machines with conductor layout and slotting effect," *IEEE Trans. Magn.*, Vol. 52, No. 8, 8107307, Aug. 2016.
14. Barcaro, M. and N. Bianchi, "Air-gap flux density distortion and iron losses in anisotropic synchronous motors," *IEEE Trans. Magn.*, Vol. 46, No. 1, 121–126, Jan. 2010.
15. Wallin, M., J. Bladh, and U. Lundin, "Damper winding influence on unbalanced magnetic pull in salient pole generators with rotor eccentricity," *IEEE Trans. Magn.*, Vol. 49, No. 9, 5158–5165, Sep. 2013.
16. Kurihara, K., "Effects of damper bars on steady-state and transient performance of interior permanent-magnet synchronous generators," *IEEE Trans. Ind. Appl.*, Vol. 49, No. 1, 42–49, Jan.–Feb. 2013.
17. Wang, L. K., F. Y. Huo, W. L. Li, Y. H. Zhang, Q. Li, Y. Li, and C. W. Guan, "Influence of metal screen materials on 3-D electromagnetic field and eddy current loss in the end region of turbogenerator," *IEEE Trans. Magn.*, Vol. 49, No. 2, 939–945, Feb. 2013.